https://doi.org/10.5194/essd-2026-488
Preprint. Discussion started: 17 August 2026

Open Access Earth System Science Data Discussions

Generating a 30 m resolution annual forest litterfall production dataset across China during 2000-2024

Xiyue Miao[1], Qi Xie[1], Luwei Feng[1], Yujie Dou[2], Feng Tian[1,3]

[1]Hubei Key Laboratory of Quantitative Remote Sensing of Land and Atmosphere, School of Remote Sensing and Information Engineering, Wuhan University, Wuhan, China
[2]Key Research Institute of Yellow River Civilization and Sustainable Development, Henan University, Kaifeng, China
[3]Perception and Effectiveness Assessment for Carbon-neutrality Efforts, Engineering Research Center of Ministry of Education, Wuhan, China

Correspondence to: Luwei Feng (lwfeng@whu.edu.cn)

Abstract. Forest litterfall links aboveground vegetation dynamics with belowground biogeochemical processes and plays an important role in soil microclimate regulation, erosion protection, and wildfire risk assessment. However, long-term, fine-resolution maps of litterfall production remain limited. Here, we compiled litterfall observations from the Chinese Ecosystem Research Network and published literature, and developed a spatial matching scheme to account for coordinate uncertainty in linking field measurements with remote sensing predictors. We integrated Landsat-derived spectral features, climatic variables, and topographic factors into a Random Forest model to generate annual 30 m forest litterfall production maps for China from 2000 to 2024. The model performed well for independent testing samples, with an R^2 of 0.72, and the resulting 30 m product captured finer spatial heterogeneity than coarser-resolution products, particularly in fragmented forests and along forest edges. In 2024, mean forest litterfall production across China was 397 g m^{-2}, with higher values generally found at lower latitudes and in evergreen forests. From 2000 to 2024, litterfall production increased across approximately 75% of China ' s forest areas, leading to an overall increase in national total litterfall input. Precipitation showed the strongest association with interannual litterfall variations, particularly in northeastern China, whereas temperature-related associations were more pronounced in southern and northwestern China. These results provide new spatial evidence for understanding forest litterfall dynamics and support improved representation of litter inputs in carbon and nutrient cycling assessments.

1. Introduction

Forest litterfall, defined as plant material naturally shed onto the ground, including leaves, twigs, flowers, fruits, and bark, is a fundamental component of forest ecosystems (Giweta, 2020). It plays a key role in carbon, nutrient, and energy cycling by linking aboveground vegetation to belowground soil processes (Freschet et al., 2013). Through faunal fragmentation, leaching, and microbial decomposition, litterfall is gradually transferred into the soil system, facilitating soil organic matter accumulation and nutrient turnover (Giweta, 2020). The litter layer covering the forest floor further moderates soil

https://doi.org/10.5194/essd-2026-488
Preprint. Discussion started: 17 August 2026

temperature variability by reducing evaporation and intercepting incoming solar radiation, while protecting topsoil from direct raindrop and subsequent erosion (Schaap and Bouten, 1997; Ogée et al., 2001). Beyond biogeochemical functions, litterfall acts as a primary surface fuel that modulates the occurrence and spread of forest fires (Li et al., 2025). Therefore, accurate spatial mapping of litterfall is critical for understanding and modeling forest ecosystem dynamics.

Ground-based observations have long provided the primary basis for quantifying litter production and understanding its temporal variability across forest ecosystems. In field studies, litterfall is typically measured using litter traps installed beneath the forest canopy to collect fallen litter components over regular intervals. The collected material is then sorted, oven-dried to constant weight, and converted to litterfall mass per unit area over a given time period. Long-term litterfall monitoring has been conducted at many sites within national and international ecosystem monitoring networks, including the U.S. Long-Term Ecological Research network (LTER), the Integrated Carbon Observation System in Europe (ICOS) (Gielen et al., 2018), and the Chinese Ecosystem Research Network (CERN). In addition, litterfall production has been measured by a number of individual studies across different regions and time periods, providing an important source of site-level observations (Shen et al., 2019).

This ground-based approach provides direct and relatively accurate estimates of litter input and has supported extensive research on temporal variability and spatial differences in forest litterfall. For example, Zhang et al. (2014) collected more than 400 litterfall observations from the existing literature and used them to investigate seasonal litterfall patterns across different forest types. Zhang et al. (2025) conducted litterfall monitoring in five representative tropical forest types on Hainan Island, China, and analyzed differences in litterfall production among vegetation types and their relationships with community properties. However, such measurements are labor-intensive, time-consuming, site-specific, and spatially sparse (Hu and Huang, 2019; Wang et al., 2016). Moreover, differences in sampling interval, and observation duration can reduce the comparability of datasets collected at different sites (Estes et al., 2018). Consequently, although ground observations remain indispensable for validation, they are insufficient for capturing the spatial heterogeneity and long-term dynamics of litterfall at regional to national scales (Shen et al., 2019; Wang et al., 2016)

Establishing statistical relationships at observation sites and extrapolating them to unsampled areas provides an effective way to generate spatially continuous forest litterfall production data. Climate conditions are closely associated with litterfall production and have therefore been widely used as predictors in litterfall modeling (Liu et al., 2024). More specific vegetation attributes, such as species composition and growth condition, are also important determinants of litterfall, but their use in large-scale mapping remains limited by the lack of spatially continuous and publicly available datasets (Shen et al., 2019; Jia et al., 2016). In this context, spectral information derived from remote sensing imagery offers a major advantage, as it can effectively capture vegetation condition while providing spatially continuous observations with repeated temporal coverage (Defries, 2008). As a result, remote sensing data have increasingly been used in litterfall estimation. For

https://doi.org/10.5194/essd-2026-488
Preprint. Discussion started: 17 August 2026

example, Zhao et al. (2022) combined MODIS-derived spectral information with climate and soil variables to estimate annual litterfall in China at 1 km spatial resolution from 2000 to 2019.

However, existing remote sensing based litterfall mapping studies still have several limitations. First, the spatial resolution of currently available litterfall products remains too coarse to capture local heterogeneity associated with forest fragmentation and variation in forest types. Second, litterfall observations are compiled from diverse sources, and issues such as non-forest site locations and missing monthly records are common, yet existing studies often lack consistent quality control and preprocessing of these field data. Third, the geographic coordinates of some ground observations are insufficiently accurate, making it difficult to establish reliable spatial matches between site-based litterfall measurements and remotely sensed or environmental predictors. This issue has received limited attention in previous studies, but it can introduce mismatches and additional uncertainty into model development.

In this study, we integrated litterfall observations from CERN and published literature, and developed a complete preprocessing workflow, including missing-value imputation and spatial matching, to construct a ground-based litterfall dataset suitable for modeling. We then combined Landsat imagery with climatic and topographic variables and applied a Random Forest model to generate annual litterfall datasets for China at 30 m spatial resolution from 2000 to 2024. Using this long-term, higher-resolution dataset, we further characterized the spatial distribution and temporal dynamics of litterfall and examined its relationships with climatic factors.

2. Data

2.1 Litterfall production data

In this study, litterfall production was expressed as the dry mass of litterfall per unit ground area, in units of g m^{-2}. The litterfall production data were compiled from two sources: CERN and published literature.

Litterfall measurements are available at a subset of national forest ecosystem research stations within the CERN. The CERN observation system is hierarchically organized, with each station comprising one or more observation sites that represent different vegetation types, such as arbor forests, shrublands, and herbaceous communities. Within each observation site, separate sampling plots are established for different ecological variables. For litterfall monitoring, multiple litter traps are installed within the corresponding litterfall measurement plot to account for local spatial variability. Litterfall samples are collected monthly, oven-dried, and converted to dry mass per unit area. Trap-level measurements are then averaged to provide a representative estimate of litterfall for each observation site.

https://doi.org/10.5194/essd-2026-488
Preprint. Discussion started: 17 August 2026

In addition, we used a published site-based dataset of annual litterfall from Jia et al. (2016), which integrates observations from numerous previous studies and includes 904 records collected between 1970 and 2014. Each record represents either multi-year averages or observations spanning multiple years.

2.2 Land cover data

The GLC_FCS30D dataset provides a long-term global land cover record at 30 m spatial resolution for the period 1985-2022 (Zhang et al., 2024). Its hierarchical classification scheme includes nine major land cover types at the first level, with an overall accuracy of 80.9%. Annual forest layers derived from this dataset were used to constrain tree litterfall estimates to forested areas. For years beyond 2022, the 2022 forest mask was applied due to the absence of updated land cover data.

2.3 Satellite imagery

Landsat series provides global 30 m observations, with each satellite having a revisit interval of 16 days (Wulder et al., 2016; Roy et al., 2014). The dataset used in this study includes observations from Landsat 5 Thematic Mapper, Landsat 7 Enhanced Thematic Mapper Plus, Landsat 8 Operational Land Imager, and Landsat 9 Operational Land Imager-2 sensors, which together form a consistent medium-resolution record of land surface conditions.

Surface reflectance data were obtained from the Google Earth Engine platform, where atmospheric correction had already been applied. To ensure data consistency and quality, integer-encoded reflectance values were converted to physical reflectance following the guidelines from United States Geological Survey, spectral differences between sensors were corrected using band-wise linear regression (Roy et al., 2016), and cloud and shadow contamination were removed using the QA_PIXEL band derived from the CFMask algorithm (Foga et al., 2017). In this study,we included both the original spectral bands and spectral indices derived from them.

2.4 Meteorological data

TerraClimate is a global climate dataset that provides monthly estimates of climatic variables and surface water balance conditions at a spatial resolution of approximately 4 km for the period 1958-2024 (Abatzoglou et al., 2018). The dataset is generated using climatically aided interpolation method, integrating high-resolution WorldClim dataset with coarser-resolution, time-varying climate data from CRU Ts4.0 and the Japanese 55-year Reanalysis (Harris et al., 2020; Kobayashi et al., 2015; Fick and Hijmans, 2017). In this study,we included precipitation, maximum temperature, and minimum temperature.

2.5 Topographic data

The Shuttle Radar Topography Mission V3 dataset, provided by National Aeronautics and Space Administration, is a global digital elevation model (DEM) derived from synthetic aperture radar observations at a spatial resolution of 30 m. In this

https://doi.org/10.5194/essd-2026-488
Preprint. Discussion started: 17 August 2026

study, we used elevation data, together with slope and aspect derived from the DEM, to characterize topographic conditions (Farr et al., 2007).

3. Methodology

Figure 1 shows the workflow for forest litterfall production mapping, which consists of four main components: litterfall data processing, spatial matching of litterfall observations under location uncertainty, feature construction, and mapping and analysis.

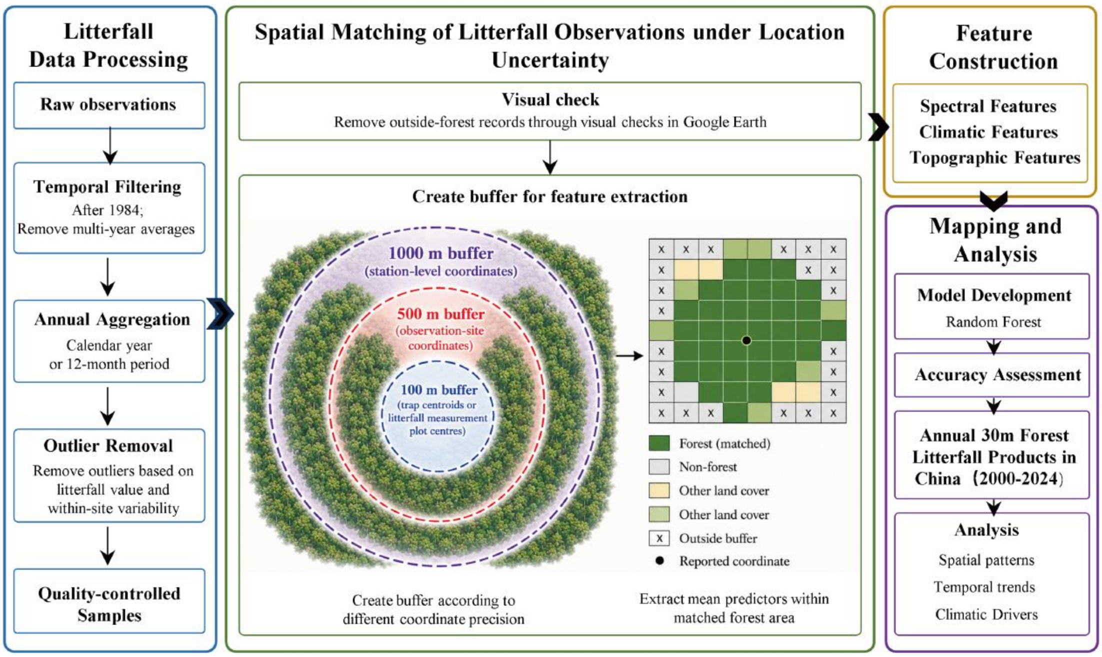

Figure 1: Workflow for mapping forest litterfall production

3.1 Litterfall data processing

To ensure consistency with the Landsat imagery, only litterfall records collected after 1984 were retained. Observations reported as multi-year averages without annual resolution were excluded, whereas records providing either annual litterfall values or monthly litterfall measurements for more than six months within a year were included. For records with missing monthly values, gaps were filled using observations from the same month in the nearest available year at the same site. Monthly litterfall values were then aggregated to annual totals, either following the calendar year or a continuous 12-month period, depending on the temporal coverage of the original observations.

Because litterfall measurements are labor-intensive and subject to both natural and anthropogenic disturbances, such as litter loss caused by wind, some observations may deviate substantially from realistic values (Zhang et al., 2014; Yang et al.,

https://doi.org/10.5194/essd-2026-488
Preprint. Discussion started: 17 August 2026

2017). To reduce the influence of such biases, we first removed outliers falling outside a plausible range of annual litterfall production (Zhang et al., 2014), defined here as less than 100 or greater than 3000 g m^{-2}. We further constrained within-site interannual variability based on the empirical observation that annual litterfall production within the same forest type generally varies by less than 300 g m^{-2} (Jia et al., 2020). For sites exceeding this threshold, we iteratively removed the yearly value farthest from the site median until the remaining within-site variability was below 300 g m^{-2}. These procedures ensured that the processed annual litterfall data were both reliable and representative at the site level, thereby providing a robust basis for subsequent large-scale modeling. After all filtering and quality-control procedures, 384 records were retained for further analysis (Fig. A3).

3.2 Spatial matching of litterfall observations under location uncertainty

A key challenge in linking field-based litterfall observations with features is the location uncertainty of the reported geographic coordinates. Litterfall measurements are typically obtained by averaging observations from multiple litter traps within a litterfall measurement plot. However, in many cases, the coordinates provided represent the centroid of multiple traps or the centre of the litterfall measurement plot. In other cases, particularly for CERN observations, the reported coordinates may refer to the observation site or even the ecosystem research station. As a result, directly extracting spatial predictors at the reported latitude and longitude may introduce a mismatch between the field measurement and the features.

To reduce this mismatch, we developed a spatial matching scheme that accounts for the positional precision of each litterfall record. First, all field locations were visually inspected using high-resolution imagery in Google Earth. Records whose reported coordinates clearly fell outside forests were excluded from further analysis. For each retained record, a circular buffer was generated around the reported coordinate, with the buffer radius determined by coordinate precision: 100 m for trap centroids or litterfall measurement plot centres, 500 m for observation-site coordinates, and 1000 m for station-level coordinates. Within each buffer, only forest pixels were retained and used as the matched area for the corresponding litterfall observation. Features were then averaged within this matched area and linked to the field litterfall record.

3.3 Feature construction

We constructed three groups of predictor variables, including spectral, climatic, and topographic features. Spectral features were derived from Landsat imagery and included the original blue, green, near-infrared (NIR), shortwave infrared 1 (SWIR1), and shortwave infrared 2 (SWIR2) bands, as well as four commonly used spectral indices: the normalized difference water index (NDWI), bare soil index (BSI), normalized difference built-up index (NDBI), and normalized difference vegetation index (NDVI). Given the limited number of valid observations within some years, these spectral variables were summarized using the annual median. To further characterize intra-annual vegetation dynamics, annual NDVI variability was quantified as the difference between the 85th and 15th percentiles of NDVI within each year. Climatic features included precipitation, daily maximum temperature, and daily minimum temperature. To capture seasonal variability

https://doi.org/10.5194/essd-2026-488
Preprint. Discussion started: 17 August 2026

within each year, these climatic variables were aggregated to quarterly values using the median. Topographic features included elevation, slope, and aspect.

3.4 Model development and accuracy assessment

Considering its robustness in handling complex and nonlinear relationships (Cutler et al., 2007), the Random Forest algorithm was used to model litterfall production. Model performance was assessed using the coefficient of determination (R2), root mean square error (RMSE), and mean absolute error (MAE). To obtain stable and reliable estimates of model accuracy, ten-fold cross-validation was performed, with each fold used as the test set and the remaining folds used for training. The reported training and testing performance represent the mean values across all folds. Finally, a model was trained using all available samples and applied to generate the litterfall production maps.

4. Results

4.1 Model performance

Figure 2 shows the combined training and testing results from ten-fold cross-validation. The model performed well on the training data (R2 = 0.94, RMSE = 54.0, MAE = 40.2), and maintained good predictive performance on the testing data (R2 = 0.72, RMSE = 119.5, MAE = 92.8), indicating strong robustness and generalization ability.

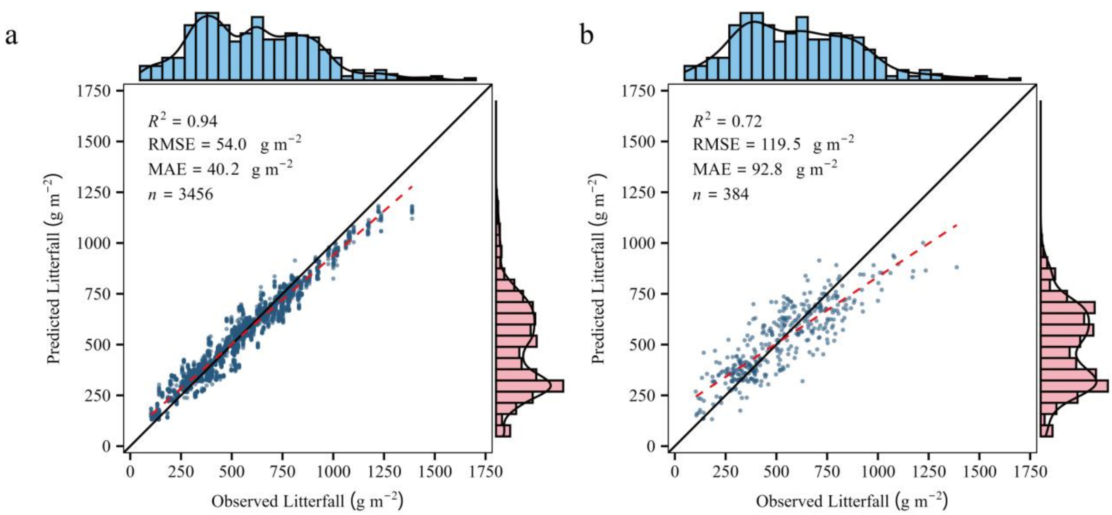

Figure 2: Model accuracy assessment based on ten-fold cross-validation on (a) training set and (b) test set.

Because no publicly available litterfall production product is currently available for comparison, we generated an additional litterfall production map for 2024 at 500 m spatial resolution using MODIS imagery, while keeping the remaining processing steps the same as those used for the 30 m product. Five representative small regions were then selected to compare the

https://doi.org/10.5194/essd-2026-488
Preprint. Discussion started: 17 August 2026

litterfall estimates derived from MODIS and Landsat imagery (Figure 3). Compared with the 500 m product, the 30 m map captures finer spatial details and more effectively represents the spatial heterogeneity of litterfall distribution. In particular, it substantially reduces the omission of litterfall signals along forest edges and within small forest patches that are frequently unresolved at coarse resolution.

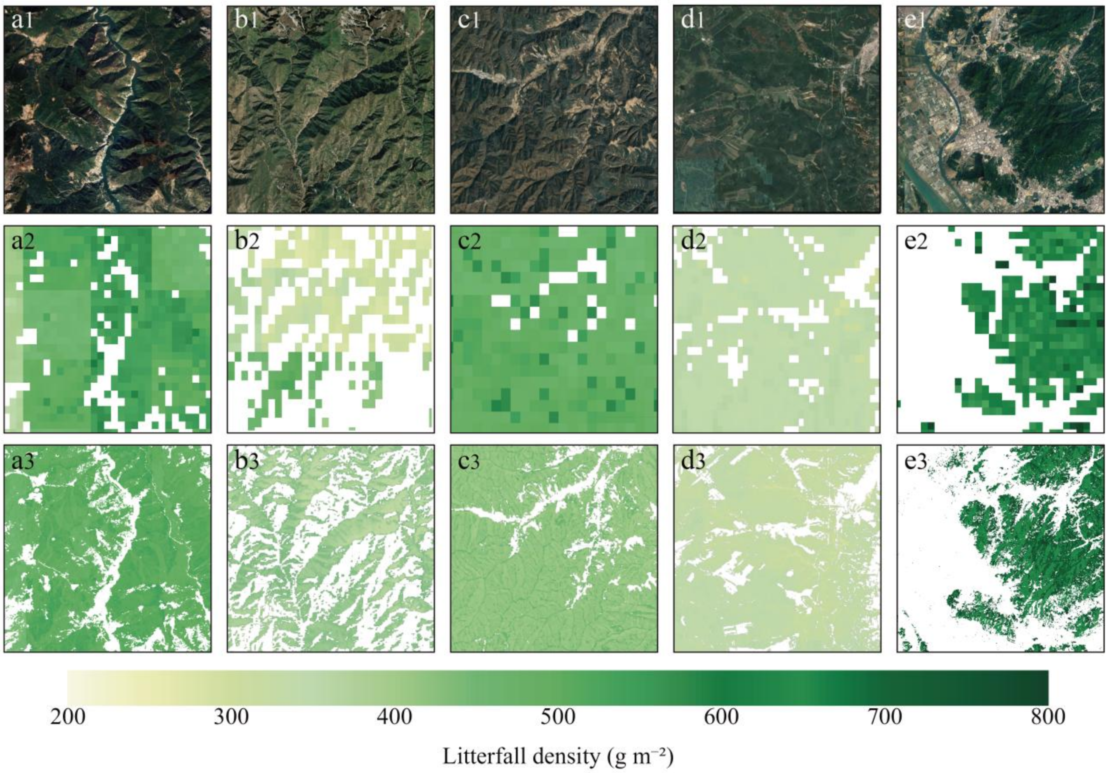

Figure 3: Multi-resolution comparison of forest litterfall production datasets in China. Rows 1–3 show Google Earth imagery, the 500 m MODIS-based litterfall product, and the 30 m litterfall product generated in this study, respectively. Columns a–e represent typical regions in Yunnan, Xinjiang, Shanxi, Heilongjiang, and Guangzhou, respectively. The coordinates indicate the upper-left corner of each comparison window: (28.8810°N, 100.8328°E), (44.1288°N, 81.7634°E), (35.8546°N, 109.0124°E), (50.1159°N, 127.1396°E), and (22.4707°N, 113.2752°E). Google Earth imagery©Google. MODIS data courtesy of NASA.

4.2 Spatial patterns of forest litterfall production

By integrating spectral, climatic, and topographic features, we developed a long-term forest litterfall production dataset for China at 30 m spatial resolution from 2000 to 2024, with the spatial distribution for 2024 shown in Fig. 4a. The mean forest litterfall production across China in 2024 was 397 g m^{-2}, with 90% of values ranging from 244 to 572 g m^{-2}. Litterfall production increased with decreasing latitude (Fig. 4b), likely because the warmer and wetter conditions at lower latitudes support higher forest productivity and consequently greater litterfall production.

https://doi.org/10.5194/essd-2026-488
Preprint. Discussion started: 17 August 2026

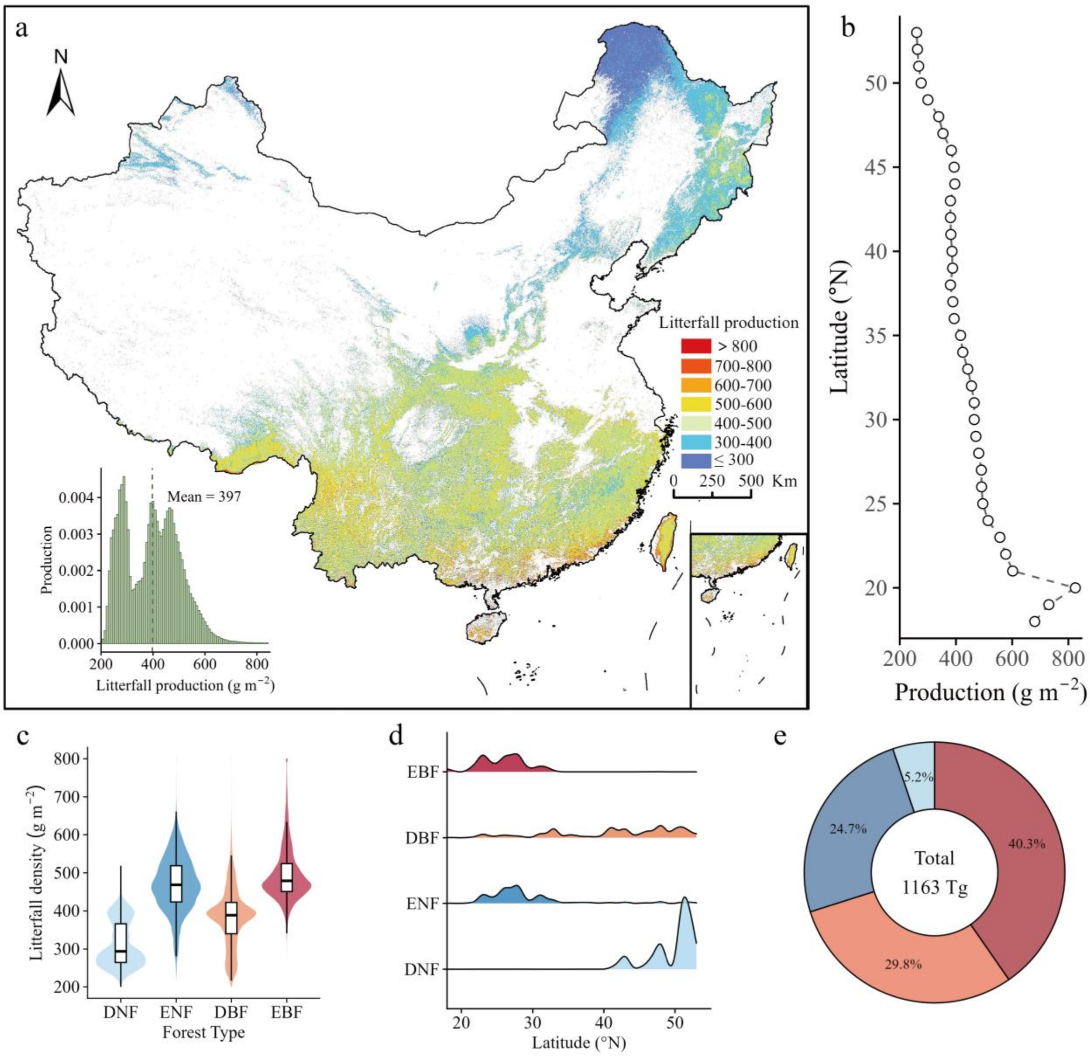

Figure 4: Spatial distribution and statistical characteristics of forest litterfall production in China in 2024. (a) Spatial distribution of forest litterfall production in 2024. (b) Distribution of forest litterfall production along the latitudinal gradient. (c) Distribution of litterfall production across forest types, including deciduous needleleaf forest (DNF), evergreen needleleaf forest (ENF), deciduous broadleaf forest (DBF), and evergreen broadleaf forest (EBF). (d) Latitudinal distribution characteristics of litterfall production across different forest types. (e) Total forest litterfall production in China in 2024 and the percentage contribution of each litter component.

Litterfall production exhibited clear spatial patterns associated with forest type. Evergreen broadleaf forests, mainly distributed in southern China (Fig. A1), showed the highest litterfall production, reaching approximately 496 g m^{-2}, and contributed the largest share of the national total 40.3%. Evergreen needleleaf forests, mainly located in southwestern China (Fig. A1), had the second highest litterfall production, with a mean value of approximately 470 g m^{-2}, accounting for 24.7% of the national total. Deciduous broadleaf forests were concentrated in northern China (Fig. A1) and contributed 29.8% of national litterfall production, largely because of their extensive distribution. In contrast, deciduous needleleaf forests were limited in area, had the lowest mean litterfall production approximately 312 g m^{-2}, and contributed only 5.2% of the total

(Fig. 4c,d). Notably, evergreen forests produced more litterfall than deciduous forests (Fig. 4e). Although this may appear to contrast with the common perception that evergreen forests shed fewer leaves, it likely reflects their continuous or asynchronous leaf turnover rather than limited leaf shedding.

4.3 Temporal trends in forest litterfall production from 2000 to 2024

Based on the annual litterfall production dataset from 2000 to 2024, we further quantified the temporal trends in forest litterfall production across China (Fig. 5a,b,c). Overall, litterfall production showed an increasing trend, with the national total increasing by 1.4T g yr^{-1}. Spatially, approximately 75% of forest areas exhibited an increasing trend, among which 39% showed a significant increase. In contrast, the remaining forest areas showed a decreasing trend, with 9% experiencing a significant decline. The areas with significant decreases were mainly concentrated in tropical forests, where 57% of the forest area showed a significant reduction in litterfall production. Tropical forests also exhibited the largest interannual variability compared with other climate zones. In addition, substantial declining areas were observed in continental and polar forest regions, where significant decreases accounted for 57% and 47% of the forest area, respectively (Fig. 5d, Fig. A2).

Except for evergreen broadleaf forests, which contained extensive areas of declining litterfall production, all other forest types showed overall increasing trends (Fig. 5e). This pattern is consistent with the climate-zone analysis (Fig. 5d), as evergreen broadleaf forests are mainly distributed in tropical and subtropical regions where declining trends were more prominent. Among all forest types, deciduous needleleaf forests exhibited the strongest increase, with an average rate of 1.9 g m^{-2} yr^{-1} and a relative increase of 16.7% in 2024 compared with 2000, the highest among the four forest types. Deciduous broadleaf forests and evergreen needleleaf forests also showed stable upward trends, with mean increases of 1.1 and 0.6 g m^{-2} yr^{-1}, respectively.

https://doi.org/10.5194/essd-2026-488
Preprint. Discussion started: 17 August 2026

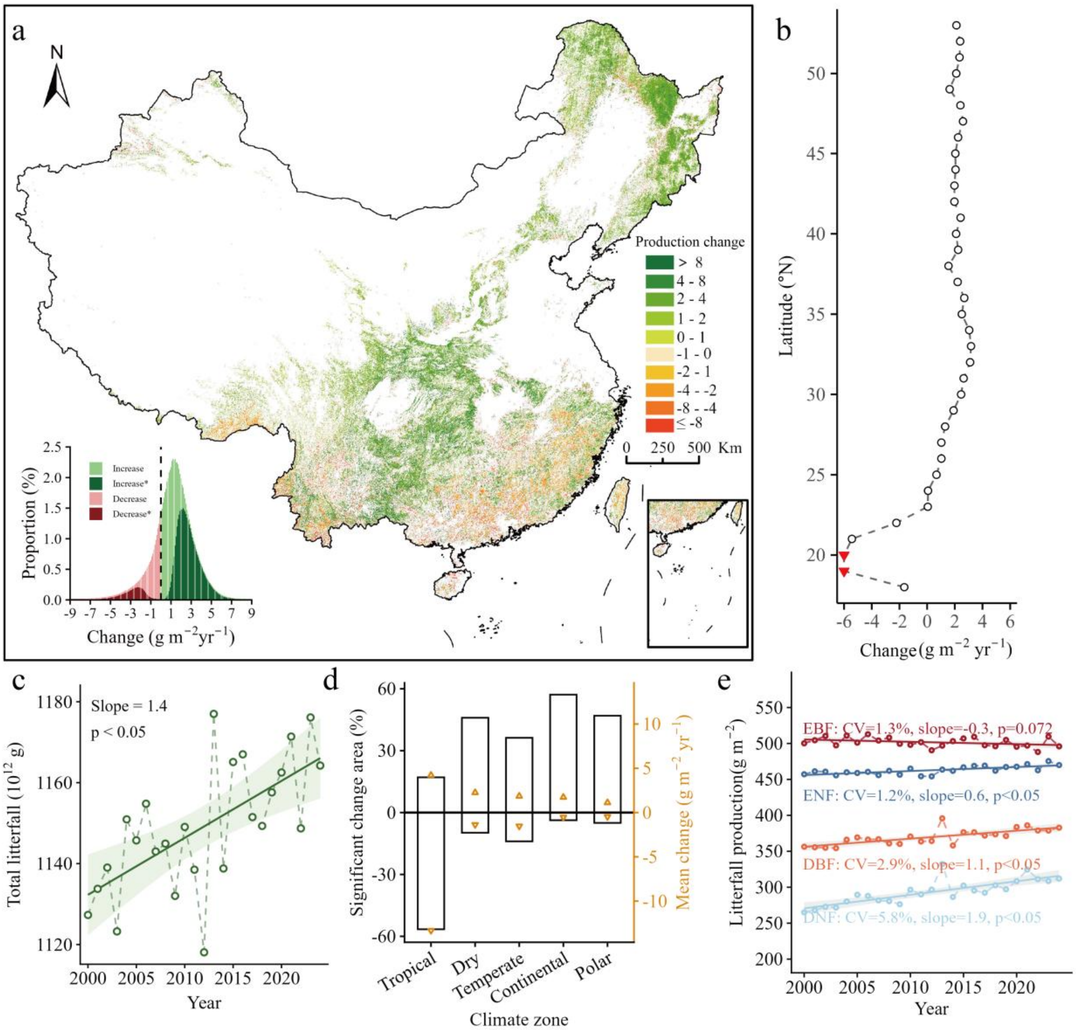

Figure 5: Temporal dynamics of forest litterfall production in China from 2000 to 2024. (a) Spatial distribution of temporal trends in forest litterfall production from 2000 to 2024. Trends were estimated using pixel-wise linear regression, and only pixels with significant changes are shown ($p < 0.05$). (b) Latitudinal distribution of annual trends in forest litterfall production. (c) Interannual variation in total forest litterfall production across China from 2000 to 2024. (d) Proportion of significantly changed area and mean rate of change in forest litterfall production across different climate zones. Triangle markers (right axis) indicate the mean absolute rate of change for significantly increasing (△) and significantly decreasing (▽) pixels (g m^{-2} yr^{-1}). (e) Trends in litterfall production for different forest types, including deciduous needleleaf forest (DNF), evergreen needleleaf forest (ENF), deciduous broadleaf forest (DBF), and evergreen broadleaf forest (EBF).

4.4 Dominant climatic factors associated with litterfall variations

Partial correlation analysis showed that precipitation was the dominant climatic factor associated with interannual variations in forest litterfall across China (Fig. 6a). Approximately 43.2% of forested areas showed the strongest association between litterfall and precipitation, with this pattern being particularly evident in northeastern China. In these regions, litterfall was

https://doi.org/10.5194/essd-2026-488
Preprint. Discussion started: 17 August 2026

positively correlated with precipitation (Fig. 6b), consistent with the concurrent increases in both precipitation and litterfall over recent decades (Fig. 5a, Fig. A5). Areas where temperature showed the strongest association with litterfall accounted for 27.5% of the forested area and were mainly distributed in southern and northwestern China. In southeastern China, litterfall was negatively correlated with temperature (Fig. 6c), suggesting that continued warming may be associated with reduced litterfall production (Fig. A4), possibly through increased evaporative demand, enhanced heat stress, or changes in vegetation growth conditions. In contrast, wind speed was identified as the dominant factor only in scattered local areas, indicating a much smaller contribution than precipitation and temperature at the national scale.

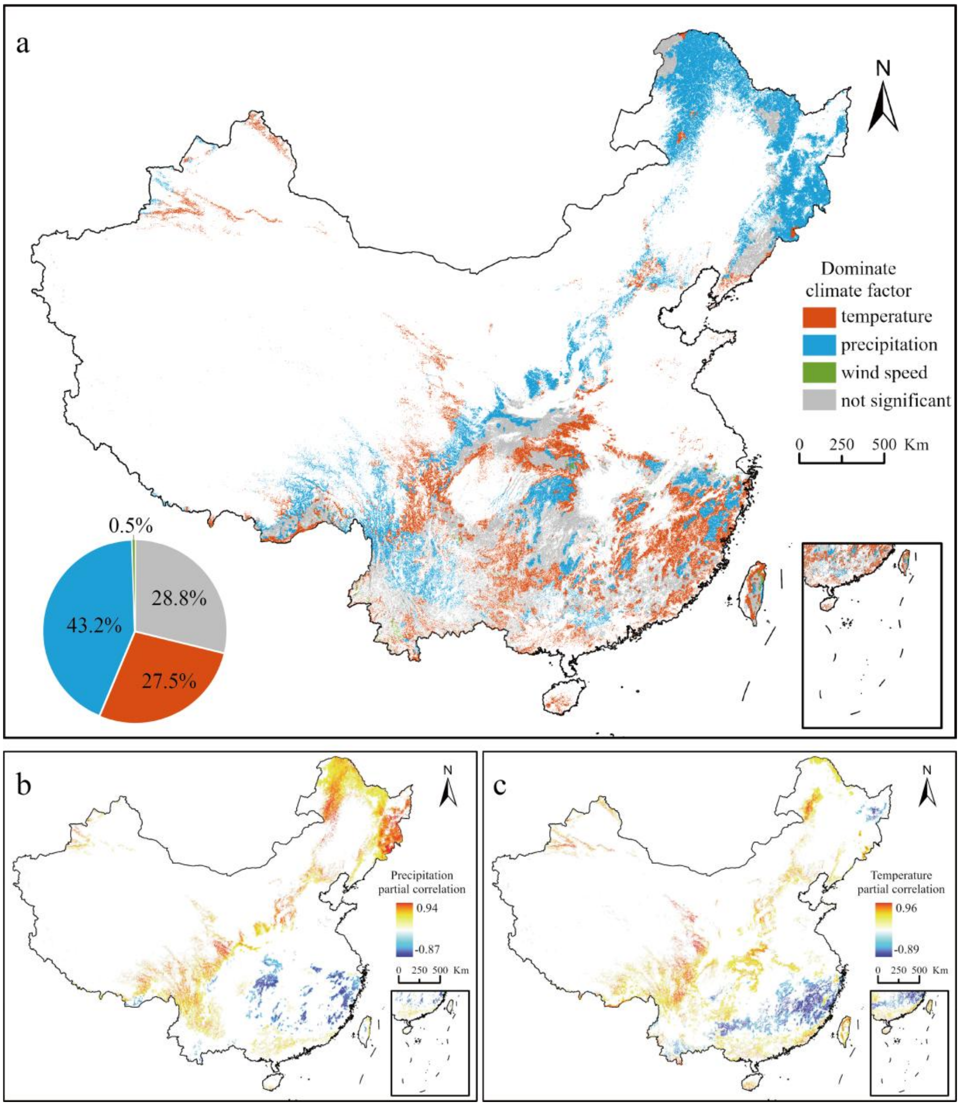

Figure 6: Effects of climatic factors on forest litterfall production in China from 2000 to 2024. (a) Spatial distribution of the dominant climatic factor exhibiting the highest statistically significant partial correlation with litterfall production. (b) Spatial distribution of significant partial correlations between litterfall production and annual total precipitation ($p < 0.05$). (c) Spatial distribution of significant partial correlation coefficients between litterfall production and annual mean temperature ($p < 0.05$) .

https://doi.org/10.5194/essd-2026-488
Preprint. Discussion started: 17 August 2026

Open Access Earth System Science Data Discussions

5. Discussion

5.1 Advantages of the developed litterfall prodcution dataset

The quality of a litterfall production dataset depends fundamentally on both the number and reliability of ground observations. In this study, we compiled a large collection of ground-based litterfall measurements from multiple sources and further improved their spatial consistency before model development. Because litterfall observations are usually reported as trap-averaged values, the provided coordinates do not always represent the exact spatial footprint of the measurements. Directly extracting features using these coordinates may therefore introduce spatial mismatch. To reduce this uncertainty, we first screened all field records using high-resolution imagery and removed samples whose reported locations were clearly outside forested areas. We then applied a spatial matching strategy based on coordinate precision, in which forest areas consistent with the recorded forest type were identified within buffers of different sizes. Features were extracted from these matched forest areas rather than from a single coordinate point. This procedure helped improve the correspondence between ground observations and environmental predictors, thereby enhancing the robustness of the training samples.

Another major advantage of the developed dataset is its 30 m spatial resolution. Compared with previous coarser-resolution products, the 30 m dataset can better represent the spatial heterogeneity of forest litterfall production. Coarse-resolution products, such as those at 500 m, often suffer from mixed-pixel effects. This problem is particularly evident in heterogeneous landscapes, where forests are fragmented or interspersed with shrublands, croplands, bare land, and built-up surfaces. Even within forested areas, a coarse pixel may contain multiple forest types, weakening the differences in litterfall production caused by vegetation composition. As a result, coarse-resolution estimates tend to smooth local variability and shift litterfall production toward spatially averaged values. By contrast, the 30 m resolution of our dataset reduces land-cover mixing and allows litterfall production to be represented more accurately at finer spatial scales.

The long-term temporal coverage further strengthens the value of this dataset. Annual litterfall production estimates from 2000 to 2024 allow spatial patterns, temporal trends, and interannual variability to be examined in a consistent framework. Together with its 30 m spatial resolution, this 25-year record provides a detailed basis for applications in forest management, carbon and nutrient cycling assessment, fire-risk evaluation, and ecosystem model benchmarking. Overall, the dataset offers a spatially explicit and temporally consistent resource for advancing the understanding of forest litterfall production and its ecological implications.

5.2 Differences in litterfall between evergreen and deciduous forests

Our results show that evergreen forests generally have higher annual litterfall than deciduous forests in both coniferous and broadleaf forest types. This pattern may seem counterintuitive, as deciduous forests exhibit a distinct and intensive leaf-shedding period in autumn (Liu et al., 2019). However, it can be explained by differences in leaf turnover strategies (Ma et

https://doi.org/10.5194/essd-2026-488
Preprint. Discussion started: 17 August 2026

al., 2023; Wright et al., 2004). Deciduous forests shed most leaves within a relatively short seasonal window, resulting in a pronounced but transient litterfall pulse (Wang et al., 2022). By contrast, evergreen forests maintain leaf replacement throughout the year, with continuous but less obvious litter inputs (Chave et al., 2010; Wang et al., 2022). Over an annual cycle, this sustained turnover may lead to greater cumulative litterfall.

Higher litterfall production does not necessarily imply faster nutrient return to soils (Zhang et al., 2014). Through microbial decomposition, litterfall links aboveground organic matter inputs with belowground soil nutrient cycling and plays an important role in ecosystem functioning and biogeochemical processes (Wardle et al., 2004). The ecological consequences of litterfall therefore depend not only on the amount of litter input, but also on litter quality and decomposability (Cornwell et al., 2008; Prescott, 2010). Deciduous litter generally has lower lignin content and lower carbon-to-nitrogen ratios, which can facilitate microbial decomposition and promote faster nutrient release (Meentemeyer, 1978; Cornwell et al., 2008). In contrast, evergreen litter is often more recalcitrant and decomposes more slowly (Liu et al., 2016). This suggests that, although deciduous forests may produce less litterfall than evergreen forests, their litter-derived nutrient release may be faster and more seasonally concentrated because of the higher decomposability of deciduous litter and the pronounced timing of leaf fall.

6. Conclusion

This study developed a 30 m annual forest litterfall production dataset for China from 2000 to 2024 by integrating quality-controlled field observations, Landsat imagery, climatic variables, topographic information, and Random Forest modeling. By explicitly addressing coordinate-related spatial mismatches, the proposed framework improved the consistency between ground measurements and spatial predictors. The resulting dataset captured fine-scale spatial heterogeneity that is often obscured in coarse-resolution products and revealed clear spatial differences among forest types and climate zones. Forest litterfall production generally increased across China over the past 25 years, reaching a national mean of 397 g m^{-2} and a total litterfall input of 1163 Tg in 2024. Evergreen forests produced more litterfall than deciduous forests, with evergreen broadleaf forests contributing the largest share of total forest litterfall production. Precipitation showed the strongest association with interannual litterfall variations, particularly in northeastern China, whereas temperature-related associations were more evident in southern and northwestern China. Overall, the developed dataset provides a spatially detailed and temporally consistent basis for investigating forest litterfall dynamics, carbon and nutrient cycling, and climate-related changes in ecosystem functioning.

https://doi.org/10.5194/essd-2026-488
Preprint. Discussion started: 17 August 2026

Appendix A

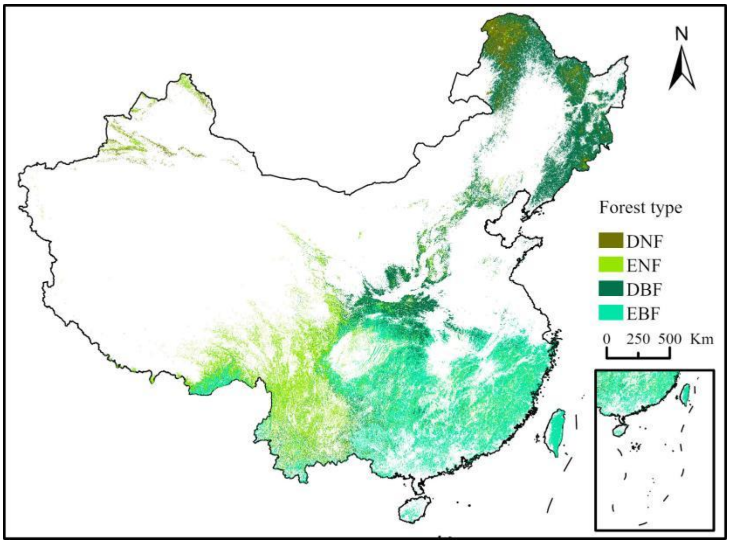

Figure A1: Spatial distribution of forest types derived from the 2024 GLC_FCS30D land cover product. The forest is classified into four major forest functional types, including deciduous needleleaf forest (DNF), evergreen needleleaf forest (ENF), deciduous broadleaf forest (DBF), and evergreen broadleaf forest (EBF). Mixed forest types are not included due to their low spatial coverage and fragmented distribution in the study area.

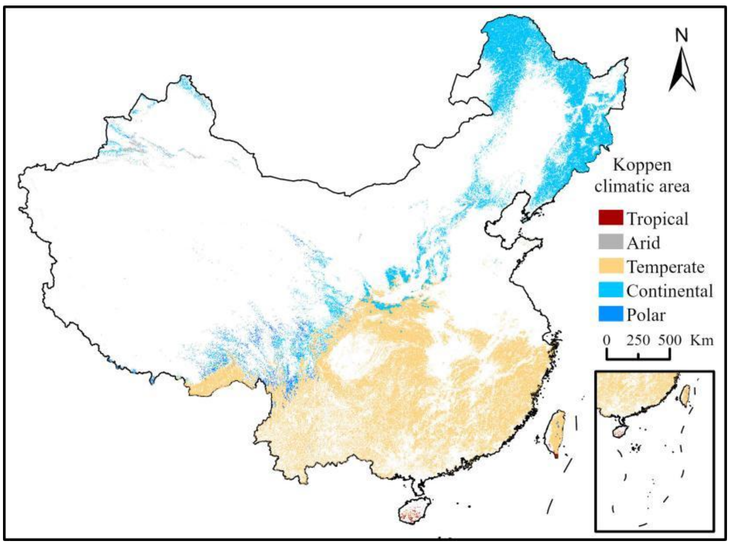

Figure A2: Spatial distribution of climate zones in China based on the Köppen–Geiger climate classification system

https://doi.org/10.5194/essd-2026-488
Preprint. Discussion started: 17 August 2026

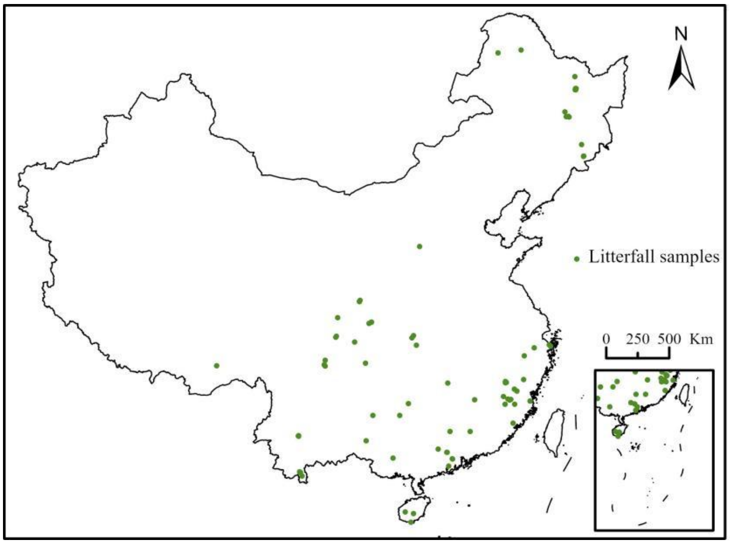

Figure A3: Spatial distribution of the final litterfall sample dataset in China (n = 384).

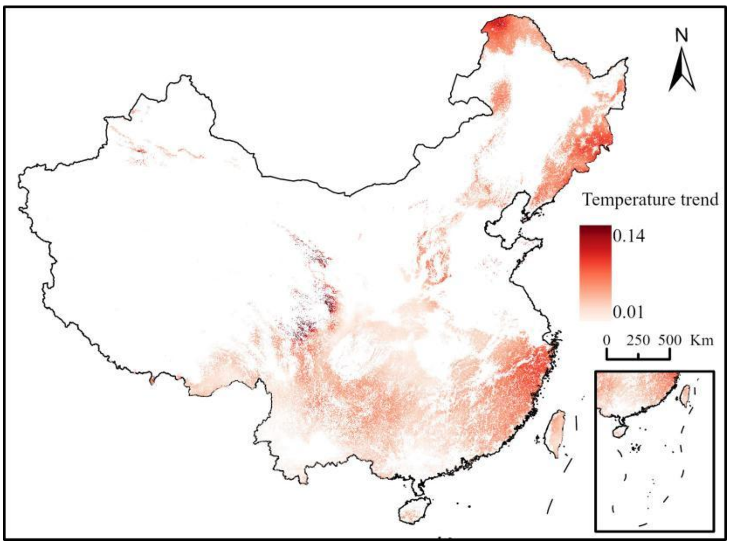

340

Figure A4: Trend of mean annual temperature (2000–2024, °C) based on linear regression. Only pixels with statistically significant trends ($p < 0.05$) are shown.

https://doi.org/10.5194/essd-2026-488
Preprint. Discussion started: 17 August 2026

Open Access Earth System Science Data Discussions

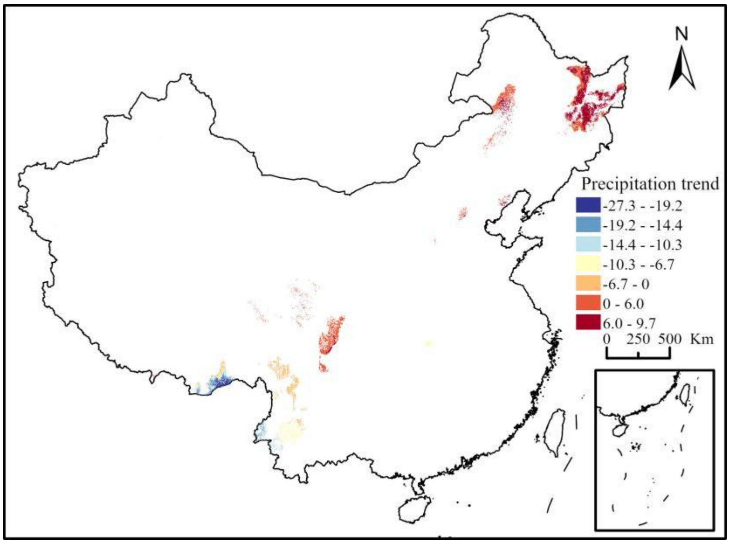

Figure A5: Trend of annual total precipitation (2000–2024, mm) based on linear regression. Only statistically significant trends ($p < 0.05$) are displayed.

Data availability

The 2024 China forest litterfall production dataset can be interactively previewed through a dedicated Google Earth Engine web application at https://mxymxy2.projects.earthengine.app/view/forest-litterfall-production-in-chinayear2024.The downloadable dataset generated in this study has been deposited in Zenodo and is publicly available at https://doi.org/10.5281/zenodo.20783253 (Miao and Feng, 2026).

Author contributions

Xiyue Miao curated the data, developed the methodology, and wrote the original draft. Qi Xie contributed to data curation and manuscript review and editing. Luwei Feng designed the study, contributed to writing the original draft, and revised the manuscript. Yujie Dou contributed to manuscript review and editing. Feng Tian designed the study and revised the manuscript.

Competing interests

The authors declare that they have no known competing financial interests or personal relationships that could have appeared to influence the work reported in this paper.

https://doi.org/10.5194/essd-2026-488
Preprint. Discussion started: 17 August 2026

Disclaimer

Financial support

This work is supported by the National Key Research and Development Program of China (Grant No 2023YFF1303702) and National Natural Science Foundation of China (No. 42501435) .

References

Abatzoglou, J. T., Dobrowski, S. Z., Parks, S. A., and Hegewisch, K. C.: TerraClimate, a high-resolution global dataset of monthly climate and climatic water balance from 1958-2015, Sci Data, 5, 170191, https://doi.org/10.1038/sdata.2017.191, 2018.

Chave, J., Navarrete, D., Almeida, S., Álvarez, E., Aragão, L. E. O. C., Bonal, D., Châtelet, P., Silva-Espejo, J. E., Goret, J. Y., von Hildebrand, P., Jiménez, E., Patiño, S., Peñuela, M. C., Phillips, O. L., Stevenson, P., and Malhi, Y.: Regional and seasonal patterns of litterfall in tropical South America, Biogeosciences, 7, 43–55, https://doi.org/10.5194/bg-7-43-2010, 2010.

Cornwell, W. K., Cornelissen, J. H. C., Amatangelo, K., Dorrepaal, E., Eviner, V. T., Godoy, O., Hobbie, S. E., Hoorens, B., Kurokawa, H., Pérez-Harguindeguy, N., Quested, H. M., Santiago, L. S., Wardle, D. A., Wright, I. J., Aerts, R., Allison, S. D., Van Bodegom, P., Brovkin, V., Chatain, A., Callaghan, T. V., Díaz, S., Garnier, E., Gurvich, D. E., Kazakou, E., Klein, J. A., Read, J., Reich, P. B., Soudzilovskaia, N. A., Vaieretti, M. V., and Westoby, M.: Plant species traits are the predominant control on litter decomposition rates within biomes worldwide, Ecology Letters, 11, 1065–1071, https://doi.org/10.1111/j.1461-0248.2008.01219.x, 2008.

Cutler, D. R., Edwards Jr., T. C., Beard, K. H., Cutler, A., Hess, K. T., Gibson, J., and Lawler, J. J.: RANDOM FORESTS FOR CLASSIFICATION IN ECOLOGY, Ecology, 88, 2783–2792, https://doi.org/10.1890/07-0539.1, 2007.

DeFries, R.: Terrestrial Vegetation in the Coupled Human-Earth System: Contributions of Remote Sensing, Annual Review of Environment and Resources, 33, 369–390, https://doi.org/10.1146/annurev.environ.33.020107.113339, 2008.

Estes, L., Elsen, P. R., Treuer, T., Ahmed, L., Caylor, K., Chang, J., Choi, J. J., and Ellis, E. C.: The spatial and temporal domains of modern ecology, Nat Ecol Evol, 2, 819–826, https://doi.org/10.1038/s41559-018-0524-4, 2018.

Farr, T. G., Rosen, P. A., Caro, E., Crippen, R., Duren, R., Hensley, S., Kobrick, M., Paller, M., Rodriguez, E., Roth, L., Seal, D., Shaffer, S., Shimada, J., Umland, J., Werner, M., Oskin, M., Burbank, D., and Alsdorf, D.: The Shuttle Radar Topography Mission, Reviews of Geophysics, 45, https://doi.org/10.1029/2005RG000183, 2007.

Fick, S. E. and Hijmans, R. J.: WorldClim 2: new 1-km spatial resolution climate surfaces for global land areas, International Journal of Climatology, 37, 4302–4315, https://doi.org/10.1002/joc.5086, 2017.

Foga, S., Scaramuzza, P., Guo, S., Zhu, Z., Jr, R., Beckmann, T., Schmidt, G., Dwyer, J., Hughes, M., and Laue, B.: Cloud detection algorithm comparison and validation for operational Landsat data products, Remote Sensing of Environment, 194, https://doi.org/10.1016/j.rse.2017.03.026, 2017.

Freschet, G. T., Cornwell, W. K., Wardle, D. A., Elumeeva, T. G., Liu, W., Jackson, B. G., Onipchenko, V. G., Soudzilovskaia, N. A., Tao, J., and Cornelissen, J. H. C.: Linking litter decomposition of above- and below-ground organs to plant–soil feedbacks worldwide, Journal of Ecology, 101, 943–952, https://doi.org/10.1111/1365-2745.12092, 2013.

Gielen, B., Acosta, M., Altimir, N., Buchmann, N., Cescatti, A., Ceschia, E., Fleck, S., Hörtnagl, L., Klumpp, K., Kolari, P., Lohila, A., Loustau, D., Marañón-Jiménez, S., Manise, T., Matteucci, G., Merbold, L., Herschlein, C., Moureaux, C., Montagnani, L., and Wohlfahrt, G.: Ancillary vegetation measurements at ICOS ecosystem stations, International Agrophysics, 32, 645–664, https://doi.org/10.1515/intag-2017-0048, 2018.

Giweta, M.: Role of litter production and its decomposition, and factors affecting the processes in a tropical forest ecosystem: a review, Journal of Ecology and Environment, 44, https://doi.org/10.1186/s41610-020-0151-2, 2020.

Harris, I., Osborn, T. J., Jones, P., and Lister, D.: Version 4 of the CRU TS monthly high-resolution gridded multivariate climate dataset, Scientific Data, 7, 109, https://doi.org/10.1038/s41597-020-0453-3, 2020.

Hu, K.-T. and Huang, C.-y.: A metabolic scaling theory-driven remote sensing approach to map spatiotemporal dynamics of litterfall in a tropical montane cloud forest, International Journal of Applied Earth Observation and Geoinformation, 82, 101896, https://doi.org/10.1016/j.jag.2019.06.006, 2019.

Jia, B., Zhou, G., and Xu, Z.: Forest litterfall and its composition: a new data set of observational data from China, Ecology, 97, 1365–1365, https://doi.org/10.1890/15-1604.1, 2016.

Jia, B., Sun, H., Yu, W., and Zhou, G.: Quantifying the interannual litterfall variations in China's forest ecosystems, Journal of Plant Ecology, 13, 266–272, https://doi.org/10.1093/jpe/rtaa010, 2020.

Kobayashi, S., Ota, Y., Harada, Y., Ebita, A., Moriya, M., Onoda, H., Onogi, K., Kamahori, H., Kobayashi, C., Endo, H., Miyaoka, K., and Takahashi, K.: The JRA-55 Reanalysis: General Specifications and Basic Characteristics, Journal of the Meteorological Society of Japan. Ser. II, 93, 5–48, https://doi.org/10.2151/jmsj.2015-001, 2015.

Li, Y., Zhang, Y., Quan, X., He, B., Veraverbeke, S., Liao, Z., and Janssen, T. A. J.: Estimating forest litter fuel load by integrating remotely sensed foliage phenology and modeled litter decomposition, Remote Sensing of Environment, 317, 114526, https://doi.org/10.1016/j.rse.2024.114526, 2025.

Liu, C., Liu, Y., Guo, K., Zhao, H., Qiao, X., Wang, S., Zhang, L., and Cai, X.: Mixing litter from deciduous and evergreen trees enhances decomposition in a subtropical karst forest in southwestern China, Soil Biology and Biochemistry, 101, 44–54, https://doi.org/10.1016/j.soilbio.2016.07.004, 2016.

Liu, F., Wang, X., and Wang, C.: Autumn phenology of a temperate deciduous forest: Validation of remote sensing approach with decadal leaf-litterfall measurements, Agricultural and Forest Meteorology, 279, 107758, https://doi.org/10.1016/j.agrformet.2019.107758, 2019.

Liu, X., Feng, Y., Zhao, X., Cui, Z., Liu, P., Chen, X., Zhang, Q., and Liu, J.: Climatic drivers of litterfall production and its components in two subtropical forests in South China: A 14-year observation, Agricultural and Forest Meteorology, 344, 109798, https://doi.org/10.1016/j.agrformet.2023.109798, 2024.

Ma, H., Crowther, T. W., Mo, L., Maynard, D. S., Renner, S. S., van den Hoogen, J., Zou, Y., Liang, J., de-Miguel, S., Nabuurs, G. J., Reich, P. B., Niinemets, Ü., Abegg, M., Adou Yao, Y. C., Alberti, G., Almeyda Zambrano, A. M., Alvarado, B. V., Alvarez-Dávila, E., Alvarez-Loayza, P., Alves, L. F., Ammer, C., Antón-Fernández, C., Araujo-Murakami, A., Arroyo, L., Avitabile, V., Aymard, G. A., Baker, T. R., Bałazy, R., Banki, O., Barroso, J. G., Bastian, M. L., Bastin, J. F., Birigazzi, L., Birnbaum, P., Bitariho, R., Boeckx, P., Bongers, F., Bouriaud, O., Brancalion, P. H. S., Brandl, S., Brearley, F. Q., Brienen, R., Broadbent, E. N., Bruelheide, H., Bussotti, F., Cazzolla Gatti, R., César, R. G., Cesljar, G., Chazdon, R., Chen, H. Y. H., Chisholm, C., Cho, H., Cienciala, E., Clark, C., Clark, D., Colletta, G. D., Coomes, D. A., Valverde, F. C., Corral-Rivas, J. J., Crim, P. M., Cumming, J. R., Dayanandan, S., de Gasper, A. L., Decuyper, M., Derroire, G., DeVries, B., Djordjevic, I., Dolezal, J., Dourdain, A., Engone Obiang, N. L., Enquist, B. J., Eyre, T. J., Fandohan, A. B., Fayle, T. M., Feldpausch, T. R., Ferreira, L. V., Finér, L., Fischer, M., Fletcher, C., Fridman, J., Frizzera, L., Gamarra, J. G. P., Gianelle, D., Glick, H. B., Harris, D. J., Hector, A., Hemp, A., Hengeveld, G., Hérault, B., Herbohn, J. L., Herold, M., Hillers, A., Honorio Coronado, E. N., Hui, C., Ibanez, T. T., Amaral, I., Imai, N., Jagodziński, A. M., Jaroszewicz, B., Johannsen, V. K., Joly, C. A., Jucker, T., Jung, I., Karminov, V., Kartawinata, K., Kearsley, E., Kenfack, D., Kennard, D. K., Kepfer-Rojas, S., Keppel, G., Khan, M. L., Killeen, T. J., Kim, H. S., Kitayama, K., Köhl, M., Korjus, H., Kraxner, F., Kucher, D., Laarmann, D., Lang, M., Lewis, S. L., Lu, H., Lukina, N. V., Maitner, B. S., Malhi, Y., Marcon, E., Marimon, B. S., Marimon-Junior, B. H., Marshall, A. R., Martin, E. H., Meave, J. A., Melo-Cruz, O., Mendoza, C., Merow, C., Monteagudo Mendoza, A., Moreno, V. S., Mukul, S. A., Mundhenk, P., Nava-Miranda, M. G., Neill, D., Neldner, V. J., Nevenic, R. V., Ngugi, M. R., Niklaus, P. A., Oleksyn, J., Ontikov, P., Ortiz-Malavasi, E., Pan, Y., Paquette, A., Parada-Gutierrez, A., Parfenova, E. I., Park, M., Parren, M., Parthasarathy, N., Peri, P. L., Pfautsch, S., Phillips, O. L., Picard, N., Piedade, M. T. F., Piotto, D., Pitman, N. C. A., Mendoza-Polo, I., Poulsen, A. D., Poulsen, J. R., Pretzsch, H., Ramirez Arevalo, F., Restrepo-Correa, Z., Rodeghiero, M., Rolim, S. G., Roopsind, A., Rovero, F., Rutishauser, E., Saikia, P., Salas-Eljatib, C., Saner, P., Schall, P., Schelhaas, M. J., Schepaschenko, D., Scherer-Lorenzen, M., Schmid, B., Schöngart, J., Searle, E. B., Seben, V., Serra-Diaz, J. M., Sheil, D., Shvidenko, A. Z., Silva-Espejo, J. E., Silveira, M., Singh, J., Sist, P., Slik, F., Sonké, B., Souza, A. F., Miścicki, S., Stereńczak, K. J., Svenning, J. C., Svoboda, M., Swanepoel, B., Targhetta, N., Tchebakova, N., Ter Steege, H., Thomas, R., Tikhonova, E., Umunay, P. M., Usoltsev, V. A., Valencia, R., Valladares, F., van der Plas, F., Van Do, T., van Nuland, M. E., Vasquez, R. M., Verbeeck, H., Viana, H., Vibrans, A. C., Vieira, S., von Gadow, K., Wang, H. F., Watson, J. V., Werner, G. D. A., Westerlund, B., Wiser, S. K., Wittmann, F., Woell, H., Wortel, V., Zagt, R., Zawiła-Niedźwiecki, T., Zhang, C., Zhao, X., Zhou, M., Zhu, Z. X., Zo-Bi, I. C., and Zohner, C. M.: The global biogeography of tree leaf form and habit, Nat Plants, 9, 1795–1809, https://doi.org/10.1038/s41477-023-01543-5, 2023.

Meentemeyer, V.: Macroclimate and Lignin Control of Litter Decomposition Rates, Ecology, 59, 465–472, https://doi.org/10.2307/1936576, 1978.

Miao, X. and Feng, L.: A 30 m Forest Litterfall Production Dataset for China [dataset], https://doi.org/10.5281/zenodo.20783253, 2026.

Ogée, J., Lamaud, E., Brunet, Y., Berbigier, P., and Bonnefond, J. M.: A long-term study of soil heat flux under a forest canopy, Agricultural and Forest Meteorology, 106, 173–186, https://doi.org/10.1016/S0168-1923(00)00214-8, 2001.

Prescott, C. E.: Litter decomposition: what controls it and how can we alter it to sequester more carbon in forest soils?, Biogeochemistry, 101, 133–149, https://doi.org/10.1007/s10533-010-9439-0, 2010.

Roy, D. P., Kovalskyy, V., Zhang, H. K., Vermote, E. F., Yan, L., Kumar, S. S., and Egorov, A.: Characterization of Landsat-7 to Landsat-8 reflective wavelength and normalized difference vegetation index continuity, Remote Sensing of Environment, 185, 57–70, https://doi.org/10.1016/j.rse.2015.12.024, 2016.

Roy, D. P., Wulder, M. A., Loveland, T. R., C.E, W., Allen, R. G., Anderson, M. C., Helder, D., Irons, J. R., Johnson, D. M., Kennedy, R., Scambos, T. A., Schaaf, C. B., Schott, J. R., Sheng, Y., Vermote, E. F., Belward, A. S., Bindschadler, R., Cohen, W. B., Gao, F., Hipple, J. D., Hostert, P., Huntington, J., Justice, C. O., Kilic, A., Kovalskyy, V., Lee, Z. P., Lymburner, L., Masek, J. G., McCorkel, J., Shuai, Y., Trezza, R., Vogelmann, J., Wynne, R. H., and Zhu, Z.: Landsat-8: Science and product vision for terrestrial global change research, Remote Sensing of Environment, 145, 154–172, https://doi.org/10.1016/j.rse.2014.02.001, 2014.

Schaap, M. G. and Bouten, W.: Forest floor evaporation in a dense Douglas fir stand, Journal of Hydrology, 193, 97–113, https://doi.org/10.1016/S0022-1694(96)03201-5, 1997.

Shen, G., Chen, D., Wu, Y., Liu, L., and Liu, C.: Spatial patterns and estimates of global forest litterfall, Ecosphere, 10, e02587, https://doi.org/10.1002/ecs2.2587, 2019.

Wang, H.-C., Lin, K.-C., and Huang, C.-y.: Temporal and spatial patterns of remotely sensed litterfall in tropical and subtropical forests of Taiwan, Journal of Geophysical Research: Biogeosciences, 121, 509–522, https://doi.org/10.1002/2015JG003113, 2016.

Wang, X., Song, H., Liu, F., Quan, X., and Wang, C.: Timing of leaf fall and changes in litter nutrient concentration compromise estimates of nutrient fluxes and nutrient resorption efficiency, Forest Ecology and Management, 513, 120188, https://doi.org/10.1016/j.foreco.2022.120188, 2022.

Wardle, D. A., Bardgett, R. D., Klironomos, J. N., Setälä, H., van der Putten, W. H., and Wall, D. H.: Ecological linkages between aboveground and belowground biota, Science, 304, 1629–1633, https://doi.org/10.1126/science.1094875, 2004.

https://doi.org/10.5194/essd-2026-488
Preprint. Discussion started: 17 August 2026

Wright, I. J., Reich, P. B., Westoby, M., Ackerly, D. D., Baruch, Z., Bongers, F., Cavender-Bares, J., Chapin, T., Cornelissen, J. H. C., Diemer, M., Flexas, J., Garnier, E., Groom, P. K., Gulias, J., Hikosaka, K., Lamont, B. B., Lee, T., Lee, W., Lusk, C., Midgley, J. J., Navas, M.-L., Niinemets, Ü., Oleksyn, J., Osada, N., Poorter, H., Poot, P., Prior, L., Pyankov, V. I., Roumet, C., Thomas, S. C., Tjoelker, M. G., Veneklaas, E. J., and Villar, R.: The worldwide leaf economics spectrum, Nature, 428, 821–827, https://doi.org/10.1038/nature02403, 2004.

Wulder, M. A., White, J. C., Loveland, T. R., Woodcock, C. E., Belward, A. S., Cohen, W. B., Fosnight, E. A., Shaw, J., Masek, J. G., and Roy, D. P.: The global Landsat archive: Status, consolidation, and direction, Remote Sensing of Environment, 185, 271–283, https://doi.org/10.1016/j.rse.2015.11.032, 2016.

Yang, Y., Yanai, R. D., See, C. R., and Arthur, M. A.: Sampling effort and uncertainty in leaf litterfall mass and nutrient flux in northern hardwood forests, Ecosphere, 8, e01999, https://doi.org/10.1002/ecs2.1999, 2017.

Zhang, H., Yuan, W., Dong, W., and Liu, S.: Seasonal patterns of litterfall in forest ecosystem worldwide, Ecological Complexity, 20, 240–247, https://doi.org/10.1016/j.ecocom.2014.01.003, 2014.

Zhang, H., Zhang, T., Zhou, Y., Huang, C., Qiu, X., Feng, G., Long, W., and Ding, Y.: Litterfall production in tropical natural forests on Hainan Island: variations across vegetation types and dependence on community properties, Ecological Indicators, 177, 113759, https://doi.org/10.1016/j.ecolind.2025.113759, 2025.

Zhang, X., Zhao, T., Xu, H., Liu, W., Wang, J., Chen, X., and Liu, L.: GLC_FCS30D: the first global 30 m land-cover dynamics monitoring product with a fine classification system for the period from 1985 to 2022 generated using dense-time-series Landsat imagery and the continuous change-detection method, Earth Syst. Sci. Data, 16, 1353–1381, https://doi.org/10.5194/essd-16-1353-2024, 2024.

Zhao, X., Tang, X., Du, J., Pei, X., Chen, G., and Xu, T.: A data-driven estimate of litterfall and forest carbon turnover and the drivers of their inter-annual variabilities in forest ecosystems across China, Science of The Total Environment, 821, 153341, https://doi.org/10.1016/j.scitotenv.2022.153341, 2022.